Title
In vivo imaging assessment of targeted radionuclide therapy of neuroblastoma using small molecule PET probe targeting human norepinephrine receptor

Author
Chandi, Rupinder Kaur

Publication Date
2013

Peer reviewed|Thesis/dissertation

In vivo imaging assessment of targeted radionuclide therapy of neuroblastoma using small molecule PET probe targeting human norepinephrine receptor

by

Rupinder K Chandi

THESIS

Submitted in partial satisfaction of the requirements for the degree of

MASTER OF SCIENCE

in

Biomedical Imaging

in the

GRADUATE DIVISION

of the

UNIVERSITY OF CALIFORNIA, SAN FRANCISCO

[redacted]

Acknowledgement

This thesis has become a reality with the intellectual nourishment, professional help and encouragement of many quarters. I am thankful to Almighty for bestowing His choicest blessings on me, which has gone a long way in giving final shape to the text.

Foremost, I would like to express my sincere gratitude to my advisor Prof. Youngho Seo for his patience, continuous support and fruitful advice, which enabled me to execute the thesis research successfully and for providing me the requisite laboratory facilities. His immaculate and worthy guidance has helped me in all the time of research and writing of this thesis.

Besides my advisor, I would like to thank the rest of my thesis committee members: Prof. Henry VanBrocklin, Prof. Byron Hann, and Prof Tracy McKnight, for their encouragement, and insightful comments.

Thanks are also due to the lab managers Joseph Blecha and Melanie Regan for their selfless support and co-operation. In particular, I am grateful to Stephanie Taylor for time-to-time help during my research.

My sincere thanks also goes to Dr. Alastair Martin, Dr. David Saloner, and Robert Smith, for allowing me to show my intellect by offering me the summer internship opportunity in this program.

Last but not the least, I would like to thank my husband Raj for his affection that has always motivated me and has been a constant source of inspiration and encouragement. Words would fall short to express my beatitude towards my parents and my family for supporting me throughout my life.

In vivo imaging assessment of targeted radionuclide therapy of neuroblastoma using small molecule PET probe targeting human norepinephrine receptor

(Rupinder K Chandi)

Abstract

Purpose: Neuroblastoma is an embryonic tumor of the peripheral sympathetic nervous system. Most of neuroblastoma tumors express norepinephrine transporter (NET), which makes metaiodobenzylguanidine (mIBG), an analogue of norepinephrine, an ideal tumor specific agent for therapy, when labeled with ^{131}I. Although drug therapies of neuroblastoma are performed regularly, there is lack of accurate quantitative assessment of tumor response to the therapy. This study was carried out with the objectives: the development of a novel ^{18}F-labeled small molecule-imaging agent that targets the human NET (hNET) receptor, the establishment of a quantitative methodology to assess the therapeutic effect of [^{131}I]mIBG and the establishment of murine xenograft model with a human neuroblastoma cell line that overexpresses hNET for better mIBG uptake would fill an unmet need to further develop treatment for this disease.

Methods: In order to enhance mIBG uptake for therapy, luciferase-expressing and hNET-transduced NB1691 (NB1691-luc-hNET) cells were implanted subcutaneously and in the renal capsule of murine xenograft models. Once the tumors reached a defined volume, the mice were injected with the [^{18}F]RP-109, a NET imaging agent and scanned on the microPET/CT instrument. The xenografts were also imaged using bioluminescence to assess the viability of the cells *in vivo*.

The mice were then treated with [^{131}I]mIBG using an established protocol. Three weeks after the [^{131}I]mIBG treatment, they were re-imaged on the microPET/CT using [^{18}F]RP-109 as well as by bioluminescence. The PET images were then correlated with the bioluminescence scans as well as tumor volume measurements to assess the utility of the probe for monitoring therapy response of the tumors.

Results: The novel probe, [^{18}F]RP-109, was successfully prepared and evaluated in neuroblastoma, but no tumor uptake was observed. The treatment of neuroblastoma with [^{131}I]mIBG therapy showed a better response with higher dose of [^{131}I]mIBG. The therapeutic data obtained from the bioluminescence imaging helps to assess the effectiveness of [^{131}I]mIBG treatment of neuroblastoma model and evaluate the functional status of tumors.

Conclusion: The NET probe was successfully radiolabelled with fluorine-18 and it did not show any visible uptake in the tumors that overexpress hNET. The [^{131}I]MIBG therapy study in mouse models using bioluminescence and tumor volume measurement as follow-up showed the effective therapy at 2 mCi level, which was consistent with the estimated tumor dosimetry study performed previously.

TABLE OF CONTENTS

LIST OF FIGURES

Introduction

Neuroblastoma is the most common extracranial solid cancer of childhood, derived from the sympathetic nervous system. The peak incidence occurs during early childhood and approximately 650 new cases are diagnosed each year in the United States [1]. In general, the prognosis of this cancer is poor. Nearly half of patients present with hematogenous metastatic disease and have a 5-year event-free survival of <50% [1,2]. A majority of children with high-risk disease show *de novo* resistance or relapse after therapy. New approaches with targeted therapy may improve efficacy without increased toxicity; for example, targeted radionuclide therapy with [^{131}I]-m-iodobenzylguanidine (mIBG) represents the most effective treatment when the cancer relapses and metastasizes [2]. Although drug and other therapies including targeted radionuclide therapy such as [^{131}I]mIBG are performed regularly, there is lack of accurate quantitative assessment of therapy response. The biomarkers expressed on the neuroblastoma cells primarily include disialoganglioside (GD2)[2,8] and human norepinephrine transporter (hNET)[2,7]. The biomarker GD2 is found on over 98% neuroblastomas and has been successfully targeted with therapeutic antibodies in humans as it mediates immune destruction of the cells [2,6,8]. The human norepinephrine transporter is a 617-amino acid transmembrane protein and is 98.9% homologous to the monkey NET. The human norepinephrine transporter (hNET) is expressed on most neuroblastoma cells, making it a valid target for imaging and therapy. An imaging probe that can assess the expression of hNET in neuroblastoma tumors can be

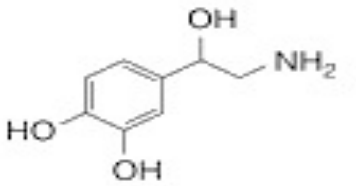

Norepinephrine

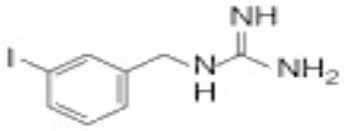

Metaiodobenzylguanidine (MIBG)

Figure 1: Similar structures of norepinephrine and MIBG, both of which are taken up via hNET

useful. M-iodobenzylguanidine (mIBG) is an aralkylguanidine norepinephrine analogue originally developed to visualize tissue of sympathetic neuronal origin, has been labeled with radioisotopes and become an essential tool for imaging (detection) as well as theraupy response monitoring [2,5]. Approximately 90% of neuroblastomas are mIBG-avid, so the labeled mIBG is now recommended as the most specific indicator for staging and response evaluation in neuroblastoma [2,5]. [^{123}I]mIBG has been used for imaging to detect tumors of the sympathetic nervous system such as neuroblastoma, whereas [^{131}I]mIBG provides a systemic form of targeted radiotherapy and has become an important tool for the diagnosis and treatment of patients with neuroblastoma. I-131 in [^{131}I]mIBG emits high-energy electrons (i.e., beta particles) with a maximum energy of 606 keV, providing therapeutic effect locally in its targets. Thus, [^{131}I]mIBG became one of standard therapies for relapsed neuroblastoma, with 30–40% response rate [5,9]. Although for [^{131}I]mIBG therapy and other drug therapies of neuroblastoma, [^{123}I]mIBG scans are performed regularly, the availability and imaging characteristics, particularly the quantitative accuracy and relatively long half-life of I-123 (13.2 hours), are not ideal. For multiple time point evaluations of therapy monitoring, short-lived radionuclide and positron emission tomography (PET) capability could provide desirable imaging

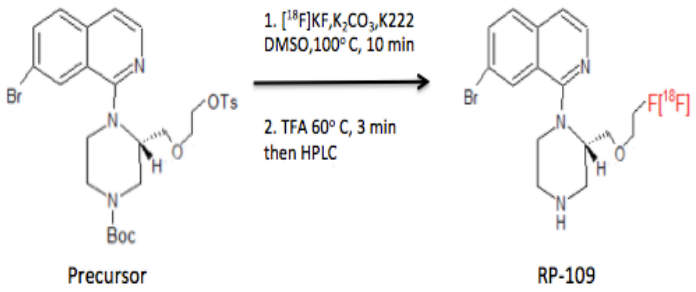

Figure 2: Radio-synthesis of [^{18}F]RP-109

properties, delivering less radiation dose each time of imaging. Fluorine -18 is, in this case, a good candidate. It is easy to produce by a medical cyclotron; decays almost exclusively (97%) via low energy (635 keV) positrons, resulting in highly resolved images. Moreover, due to the widespread use of [^{18}F]FDG, the infrastructure for its use is highly developed in medical facilities[10]. The development of a novel ^{18}F-labeled small molecule-imaging agent that targets the hNET receptor, and the establishment of a quantitative methodology to assess the therapeutic effect of [^{131}I]mIBG in a murine xenograft model of neuroblastoma would fill an unmet need for therapeutic development.

We aim to evaluate a fluorine-18 labeled NET imaging agent that targets the biomarker expressed on neuroblastoma cells, hNET in this experiment. Dr. John Gerdes at the University of Montana has developed a ^{18}F-labeled high affinity ligand for NET ([^{18}F]RP-109, Figure 2) and has validated its utility in a rhesus monkey model for imaging NET in brain [3,4]. [^{18}F]RP-109 was developed using a combination of molecular modeling and iterative structure activity optimization. It binds to NET with nanomolar affinity (Ki=1.1nM) and exhibits high selectivity (>1,000-fold greater than its binding to the closely related serotonin transporter) [3,4]. The radiosynthesis of this probe has been optimized with >98% radiochemical purity and a high specific activity of 1.8 ± 0.9 Ci/μmol[4]. Initial *in vivo* validation of the probe has been performed in a rhesus monkey model, where

PET imaging 30 minutes after probe injection revealed a distribution consistent with that of NET (brainstem > thalamus > cingulated cortex = insula > frontal cortex)[4]. This pattern could be blocked via pre-treatment with nisoxetine (1 mg/kg), a known NET inhibitor, whereas the serotonin selective inhibitor citalopram has no effect [4]. This has validated the use of [^{18}F]RP-109 as a specific imaging agent for NETs *in vivo.* However, this probe has not been investigated for any oncologic application such as imaging neuroendocrine tumors that express hNET, including neuroblastoma. So, the aim is to establish the radiosynthesis of [^{18}F]RP-109, providing access to this small-molecule PET tracer for evaluation in neuroblastoma. Hence we will use the newly synthesized probe to follow the effect of mIBG treatment on a murine xenograft model with a human neuroblastoma cell line that has been transduced with the hNET for improved mIBG uptake.

Moreover, the lack of neuroblastoma xenografts models with *in vivo* uptake of mIBG has hindered further exploration of combination therapies and also made the correlation with tumor models in these models difficult. Most previously published studies using mIBG have utilized non-neuroblastoma cell lines transduced with hNET in order to facilitate uptake. In the past, murine models of neuroblastoma or human xenograft models have rarely been used to test mIBG therapy due to poor uptake *in vivo* by many of the neuroblastoma cell lines despite hNET expression and good *in vitro* uptake [5]. For this reason, we use a murine xenograft model with a human neuroblastoma cell line that has been transduced to overexpress hNET for better mIBG uptake, to show the utility of *in vivo* imaging

validation of [^{18}F]RP-109 tumor uptake using PET/CT scans and [^{131}I]mIBG dosimetry using bioluminescence imaging.

Materials and Methods

All PET/CT imaging experiments were performed using [^{18}F]-RP-109 with the precursor provided by John Gerdes at the University of Montana. In collaboration with Dr. Weiss' group at UCSF, luciferase-expressing and hNET-transduced NB1691 (NB1691-luc-hNET) cells were implanted either subcutaneously or in the renal capsule of mice. Previous experience within our group has noted significant differences between these two xenograft models; hence we examined both of them during this study. Once the tumors reached a defined volume (100-300 mm^3), the mice were injected with the [^{18}F]RP-109 and scanned on the microPET/CT instrument. The xenografts were also imaged using bioluminescence to assess the viability of the cells *in vivo*. The mice were then treated with [^{131}I]mIBG using an established protocol. Three weeks after [^{131}I]mIBG treatment, they were re-imaged on the microPET/CT using [^{18}F]RP-109, as well as by bioluminescence. The PET images were then correlated with the bioluminescence scans as well as tumor volume measurements (when subcutaneous tumors were used for the animal model) to assess the utility of the probe. In addition, another cohort of mice was used simply for imaging, with no [^{131}I]mIBG treatment as a control group. Again PET scans were compared to bioluminescence scans and caliper measurements to obtain the therapeutic assessment data when no treatment was applied.

Synthesis of [^{18}F]-RP-109

The F-18 labeling was performed as previously published with some modifications. The fluoride was prepared by adding $^{18}F^-$ in 500 µl of H_2O to a 10% water/acetonitrile solution of K_2CO_3/K_{222} (1mg/6mg) that was then azeotropically dried with additions of CH_3CN while heating (100 ˚C) under vaccum. The precursor (~0.5 mg) was dissolved in 200 µL of dimethyl sulfoxide (DMSO) and added to the dried $^{18}F^-$. The reaction was then heated to 100 ˚C for 10 mins. Radio Thin Layer Chromatography (Radio TLC) was performed in 2:3 ethyl acetate (EtOAc)/ hexanes to confirm labeling. In the next step, the reaction mixture was diluted with 15 mL of water and loaded on to a C18 light SepPak (Waters) preconditioned with 5 mL of CH_3CN followed by 10 mL of H_2O. The SepPak was loaded with the reaction mixture diluted with water and then washed with 10 mL of water and finally eluted with 2 mL acetonitrile to give the radioactive intermediate. In the first attempt of the deprotection, 1 mL of trifluoroacetic acid (TFA) was added to 1 mL of CH_3CN containing [^{18}F] protected intermediate and heated to 60^{o}C for 10 mins. The reaction was cooled and quenched with 2 mL of 1M $NaHCO_3$ and injected into HPLC for analysis. The radioactive peak is collected and diluted with 2 mL of H_2O and reinjected. The other 1 mL of [^{18}F] protected intermediate was dried down and took up in 500 µl of TFA and heated to 60^{o}C for 10 mins. The reaction was cooled and quenched with 2.5 mL of HPLC solvent system and injected on the HPLC for analysis. The desired product was collected and diluted up with water and loaded onto a C18 light SepPak. The SepPak was washed with 5 mL of water and finally eluted in 200 uL fractions with ethanol. The fractions with the highest amount of activity were

combined and placed under N_2 flow to evaporate. Saline was added to give the final injectable solution. The final product was analyzed by RP-HPLC using UV and radiation detectors, under the following conditions: 40/60 acetonitrile/water with 0.1% TEA (pH 11.2-11.4) solvent at a flow of 4 mL/min on Gemini semi-prep C18 column at 254 nm. The purity and yield of the radiosynthesis was calculated and compared with non-radioactive standard of RP-109. The radiochemical purity was over 98% prior to administration of the labeled [^{18}F]RP-109 into the animals.

Animal Models of Neuroblastoma

The imaging and therapy was done on athymic mice implanted with hNET overexpressing NB1691 neuroblastoma cells, which had been previously modified to express the firefly luciferase protein (NB1691-luc). A total of thirty athymic mice (weighing approximately 25 g each) were implanted subcutaneously with 1.5×10^6 luciferase-expressing and hNET-transduced NB1691 (NB1691-luc-hNET) cells on the right shoulder. In addition, thirty athymic mice were implanted in the renal capsule in the left kidney with 1.5×10^6 NB1691-luc-hNET cells. The athymic mice show a visual tumor (on the right shoulder) in the subcutaneous model, whereas no visual tumor was seen in the renal capsule model (Figure 3).

Figure 3: Subcutaneous model (left) showing visual tumor and renal capsule model (right) showing no visual tumor

Animal Imaging Protocol

Preclinical PET/CT imaging utilized standard operating procedures approved by the University of California, San Francisco Institutional Animal Care and Use Committee and Laboratory Animal Resource Center. Prior to the [^{131}I]mIBG study, we enrolled three renal capsule model mice for the [^{18}F]RP-109 imaging. Since there is no palpable tumor in renal capsule model unless the tumor is very large, we assessed the presence of tumor from the bioluminescence signal. The mice were injected with the [^{18}F]RP-109 and scanned on the microPET/CT instrument. The mice received 1.7-4.2 MBq of [^{18}F]RP-109 solution in 120-200 µl volume intravenously using a custom mouse tail vein catheter with a 28-gauge needle and a 100- to 150-mm long polyethylene microtubing (0.28 mm I.D. × 0.64 mm O.D., Scientific Commodities, Inc., Lake Havasu City, AZ). The mice were imaged on a dedicated small animal PET/CT scanner (Inveon, Siemens Healthcare, Malvern, PA). The energy window for Fluorine-18 PET was set at 350-650 keV for the optimal noise equivalent count rate performance at the given administered dose levels and the scanner characteristics. Both the animals were imaged for 60 mins each using the dynamic PET scans. The CT data were acquired without removing the animals from the scanner after the PET data acquisition. The coregistration between PET and CT images was obtained using the rigid transformation matrix from the manufacturer-provided scanner calibration procedure since the geometry between PET and CT remained constant for each of PET/CT scans using the combined PET/CT scanner. Animals were anesthetized with gas isoflurane at 2% concentration mixed with medical grade oxygen. The acquisition time for PET was 3600 sec, with a timing

window of 3.432 nsec. The *in vivo* CT parameters were 120 projections of continuous rotations to cover 220° with an X-ray tube operated at 80 kVp, 0.5 mA, and 175 ms exposure time [5].

Manufacturer-provided ordered subsets expectation maximization algorithm was used for PET reconstruction that resulted in 128 × 128 × 159 matrices with a voxel size of 0.776 × 0.776 × 0.796 mm^3. The CT image was created using a conebeam Feldkamp reconstruction algorithm (COBRA) provided by Exxim Computing Corporation (Pleasanton, CA). The matrix size of the reconstructed CT image was 512×512×700 with an isotropic voxel size of 0.196 × 0.196 × 0.196 mm^3. The photon attenuation correction was performed for PET reconstruction using the coregistered CT-based attenuation map to ensure the quantitative accuracy of the reconstructed PET data [5]. Since no uptake was observed in the renal capsule model, the imaging was performed on the two subcutaneous model mice that did not undergo any therapy to see if there is any uptake in the subcutaneous model.

Tumor Uptake

Tumor and normal organ *in vivo* distribution studies were performed using the reconstructed PET/CT image data for both the renal capsule and subcutaneous models as follows. First, the AMIDE software package was used to assess the tumor uptake of [^{18}F]RP-109. For the visual representation of the tumor uptake, we took the 51- 60 min time point PET/CT images for both the models. At this point, most of the tracer uptake in other organs and tissues were cleared from the animals, and it was assumed that the [^{18}F]RP-109 is bound to the hNET-overexpressing tumors. The regions of interest (ROIs) on the coregistered CT images for each tumor and

organ were drawn, and ROIs were transferred to PET images. The same manual ROI drawing procedure was repeated using the CT images that were coregistered by applying the precalibrated rigid transformation matrix between the fixed positions of PET and CT. Once transferred, the apparent partial volume spill-outs were adjusted manually. After the ROI were drawn at the selected regions (the right shoulder in the subcutaneous model and the left renal capsule in the renal capsule model), the statistics were checked to look at the mean values and compared with the mean values of the muscle at all the different time frames. The Time Activity Curve (TAC) was evaluated to look at the standard uptake value (SUV) of the tracer in the tumor with time. Also, instead of a two-dimensional representation of mIBG uptake such as cross sectional views, a full three-dimensional volume rendering of both PET and CT overlaid was created, to look at the biodistribution of the tracer with time, using AMIDE.

[^{131}I]mIBG Therapy

[^{131}I]mIBG therapy was performed five weeks after the implantation of the hNET overexpressing NB1691 neuroblastoma cells, i.e. when the tumor reached a volume of at least 100-300 mm^3. For the therapy, thirty subcutaneous and thirty renal capsule mice were used. The thyroid was blocked with 0.250 mg/100 μL of an aqueous solution of sodium iodide administered intravenously via tail vein approximately 1 h prior to [^{131}I]mIBG injections to prevent excessive I-131 uptake. 100 μL of the [^{131}I]mIBG solution was delivered intravenously using a custom mouse tail vein catheter with a 28-gauge needle and a 100- to 150-mm long polyethylene microtubing (0.28 mm I.D. × 0.64 mm O.D., Scientific Commodities, Inc.,

Lake Havasu City, AZ). Both the models were divided into three sets of ten animals each. The first set of mice received 74 MBq (2 mCi) of [^{131}I]mIBG, the second set was given 37 MBq (1mCi) of [^{131}I]mIBG , and the third set was used simply for imaging, with no [^{131}I]mIBG treatment as a control group.

Body Weight and Tumor Measurements

The body weight measurements of the mice were conducted to assess if there was any deleterious effect to the health of mice from the tumor or bioluminescence imaging. The caliper measurements were used to calculate the tumor volumes (in case of the subcutaneous tumor models). For caliper measurements, the mouse was anesthetized and assuming the tumor was ellipsoid, the long and the short axis of the tumor was determined. Using the calipers, both axes were measured carefully without squeezing the tumor. The measurements were recorded in mm. The tumor volumes were calculated using the formula: $1/2 \times \text{long axis} \times (\text{short axis})^2$.

Bioluminescence Imaging

The D-luciferin bioluminescence imaging was used to assess the viability of cells in vivo. For the bioluminescence imaging, the Xenogen IVIS 50 machine was initialized and the nose cone was centered in the FOV. The exposure time was set to auto, bin was set to medium and the F/stop was set equal to 1. Then, 100 µL of thawed D-luciferin was injected intraperitoneally and the mouse was imaged exactly 10 mins post injection.

Statistical Analysis

Statistical analyses were performed using Excel spreadsheets. Data were expressed as average ± standard deviation (SD). The statistical significance was tested using

the unpaired t-test, in which the comparison was performed between the 2 mCi - 1 mCi and 2mCi - 0 mCi cohorts for the tumor volume change and the total flux change. The comparison was performed with the average and standard deviation values from day 14, i.e, when there was relapse after the therapy.

Results

Synthesis of [^{18}F]-RP-109

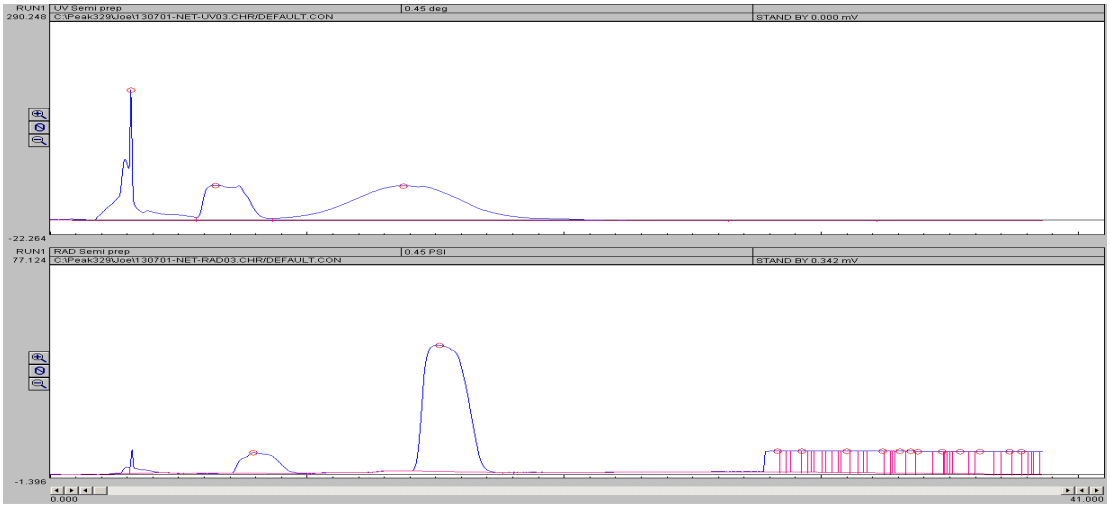

Figure 4: UV (top) and Rad (bottom) HPLC traces from the synthesis of the [^{18}F]RP-109. The x axis shows the time in minutes and the y axis are amplitudes for each detector.

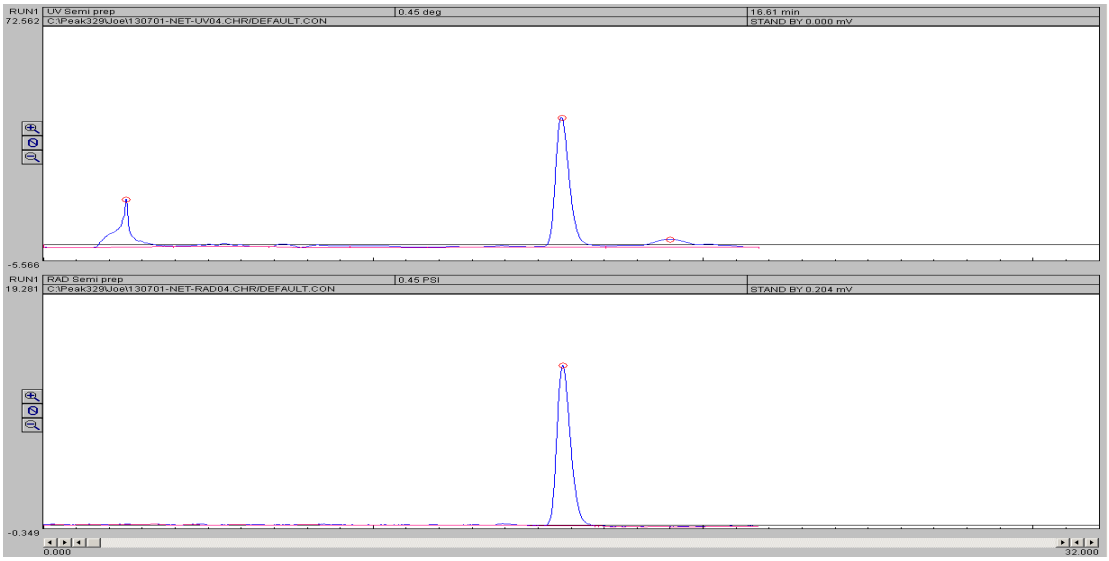

Figure 5: UV (top) and Rad (bottom) HPLC traces from the QC sample of the [^{18}F]RP-109. The x-axis shows the time in minutes and the y axis are the amplitudes for each detector.

We demonstrated that the novel probe was successfully radiolabeled for evaluation in neuroblastoma. Figure 4 shows the radio HPLC trace of the desired product coming from 14-18 minutes while the upper trace shows minimal mass coming before the tracer. Figure 5 is a quality control HPLC trace with a known amount of non-radioactive RP-109 so that we can confirm the identity of the radioactive peak that was collected from Figure 4. The purity and yield of the radiosynthesis was calculated and compared with non-radioactive standard of RP-109. The radiochemical purity was over 98% prior to administration of the labeled [^{18}F]RP-109 into the animals. The final product was analyzed by RP-HPLC using UV and radiation detectors and co-eluted at 15.4 mins (Figure 5).

[^{131}I]mIBG Therapy

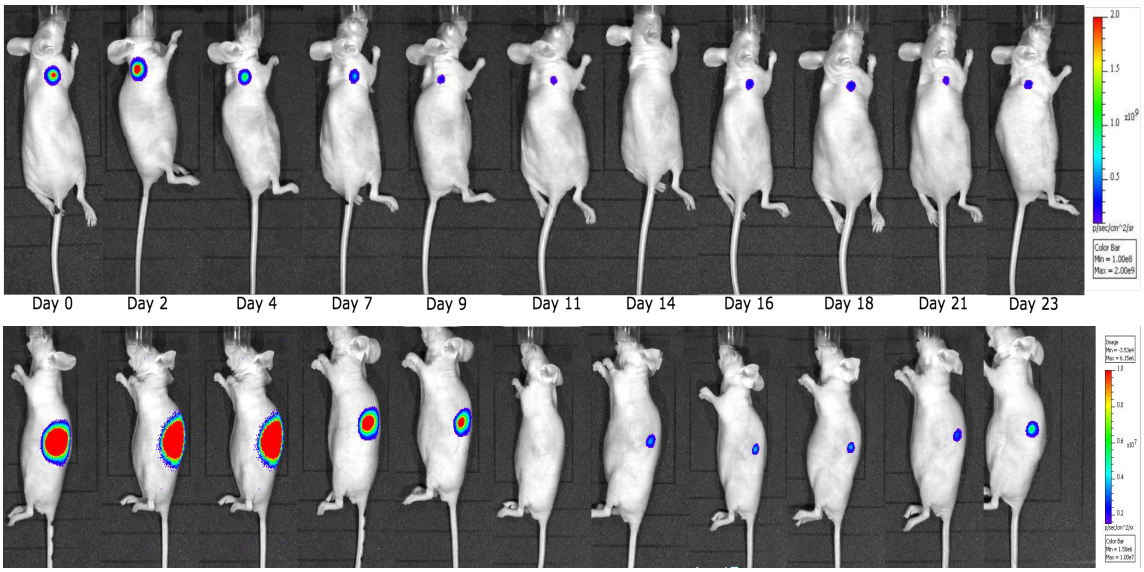

Figure 6: Bioluminescence Images showing change in the total flux after therapy in subcutaneous (top) and renal capsule (bottom) models

The change in bioluminescence signal was observed over time. There was a decrease in the total flux in the second week after mIBG therapy indicating the response to therapy, and slight increase in the total flux after day 14 shows relapse.

This pattern was observed in both the subcutaneous as well as renal capsule models (Figure 6).

Body Weight and Tumor Measurements

The body weight measurements of the animals showed that [^{131}I]mIBG administration at 1 and 2 mCi levels affect the general health of mice in the long-term . The mice in both the subcutaneous and renal capsule models show an increase in the body weight with the growth of the tumors until the therapy is applied and an observable decrease in body weight for 1.5 weeks after the therapy. After the second week, there was an increase in the body weight in mice again (Figure 7). The normalized caliper measurements of tumor volumes of the subcutaneous models show the expected trend. The first cohort of mice that received 74 MBq of [^{131}I]mIBG shows a decrease in tumor volume after 1.5 weeks followed by an observable increase in tumor volume beyond 9-10 days after treatment. In the second cohort of mice that received 34 MBq of [^{131}I]mIBG, there was decrease in tumor volume after the first week and then an increase after the second week whereas no decrease was observed in the third cohort that received 0 MBq of [^{131}I]mIBG. Therefore, the mice in the control group show no decrease in the tumor volume whereas the mice treated with the MIBG shows decreased volume of the tumor, indicating response to the therapy.

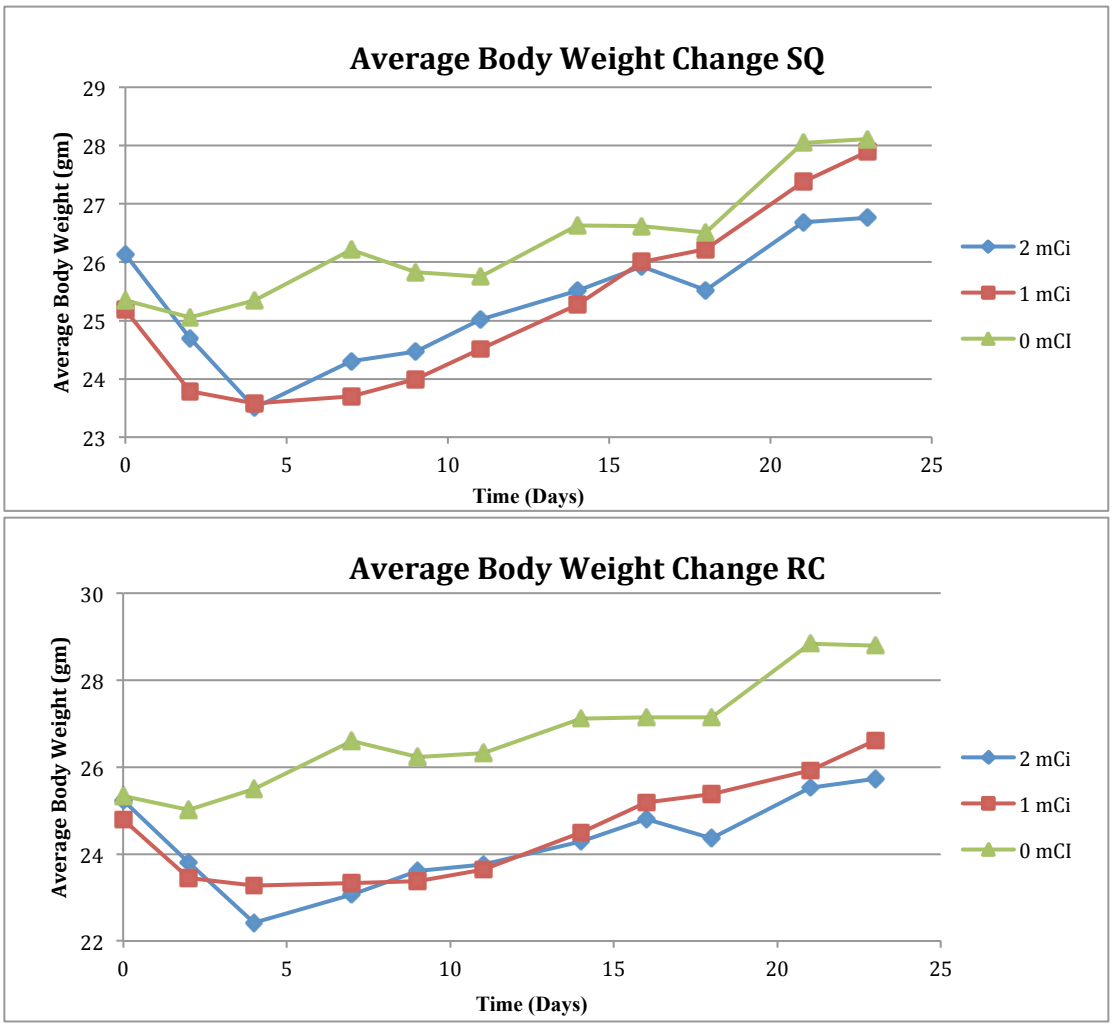

Figure 7: Average change in body weight in the subcutaneous (top) and renal capsule (bottom) model over time

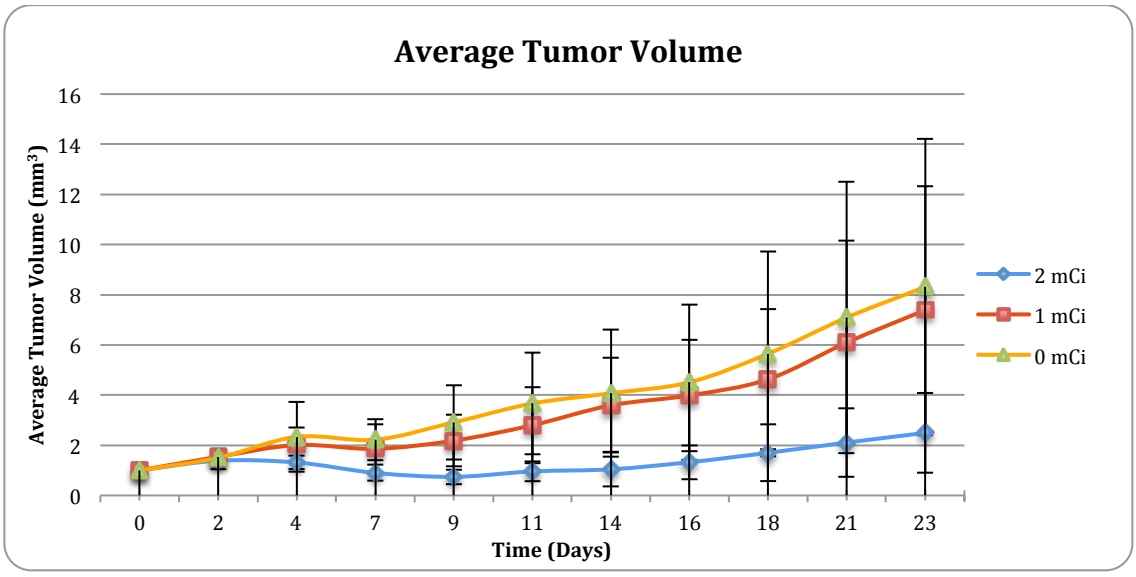

Figure 8: Average tumor volume change after therapy in the subcutaneous model

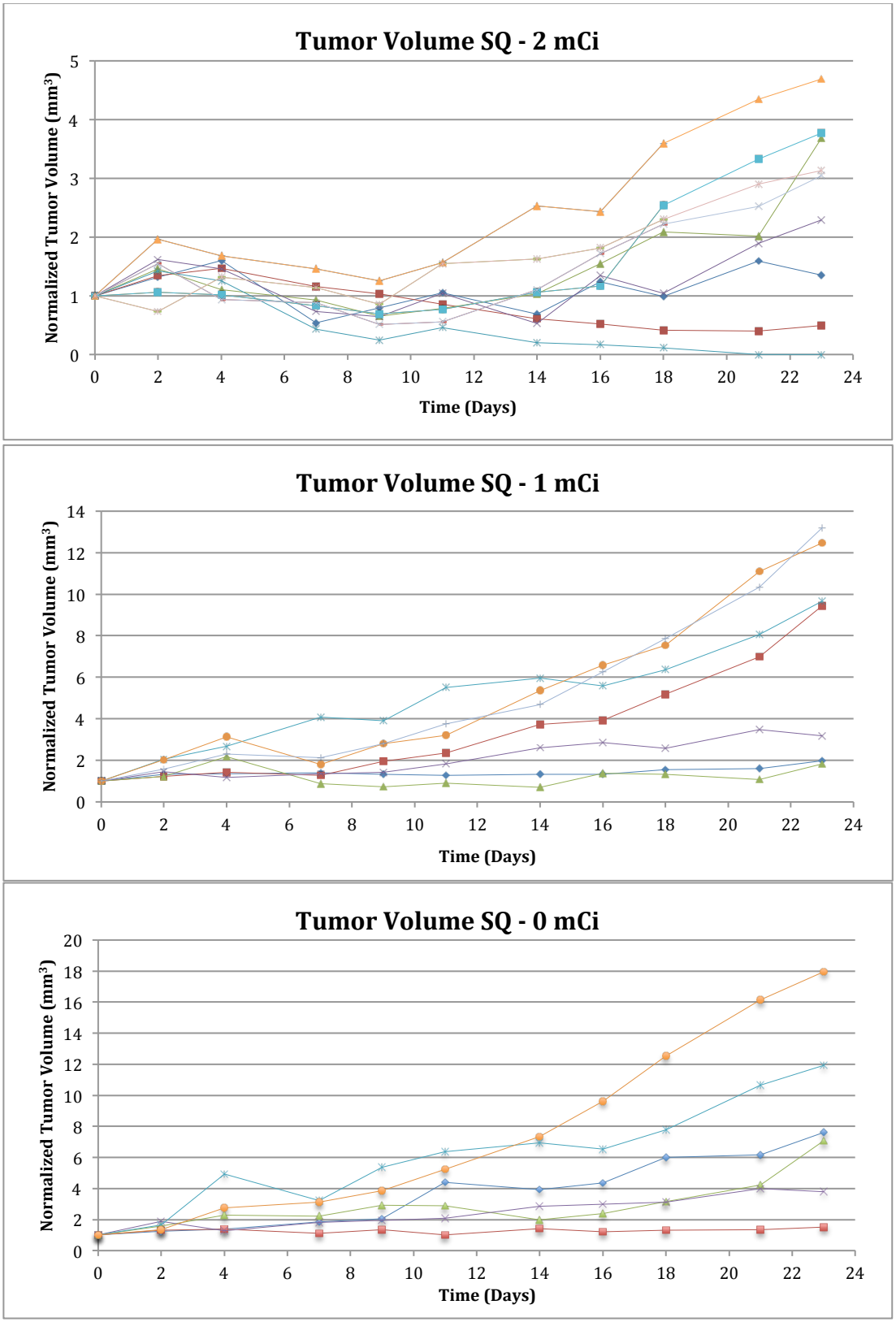

Figure 9: Change in Tumor volume per animal after [^{131}I]mIBG therapy in different cohorts of the subcutaneous model: 2mCi (top), 1mCi (middle), 0mCi (bottom)

Bioluminescence Imaging

The data obtained from bioluminescence imaging helps to assess the effectiveness of [^{131}I]mIBG treatment of a murine neuroblastoma xenograft model. The therapeutic assessment data from the bioluminescence imaging shows the change in the total flux after therapy (Figure 10). The total flux obtained from the bioluminescence imaging shows the total number of photons emitted per second. The total flux

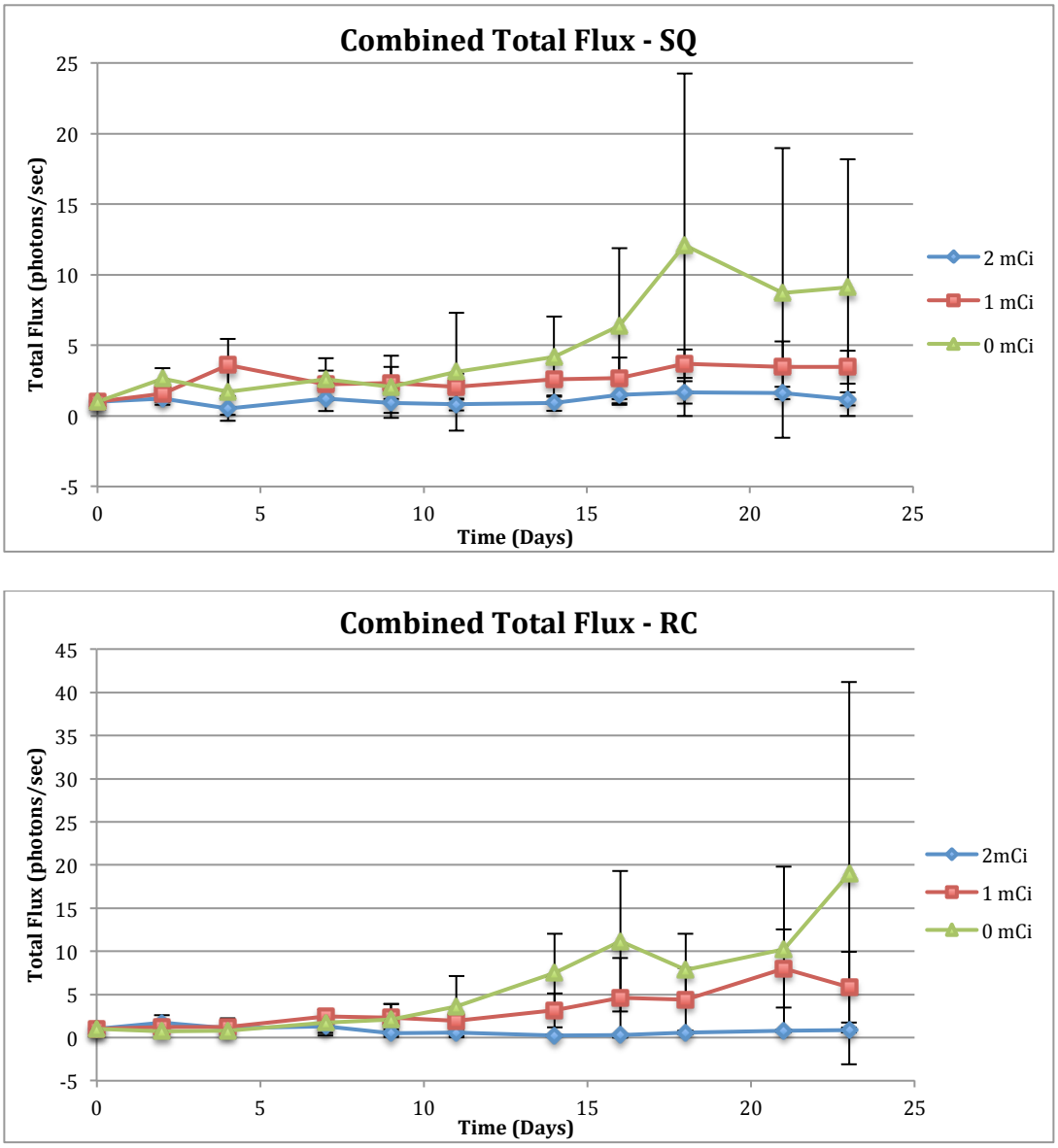

Figure 10: Combined Total Flux of all the cohorts of subcutaneous (top) and renal capsule (bottom) models

changes in the first cohort of mice that received 74 MBq (2 mCi) of [^{131}I]mIBG show a general trend of signal decrease on day 4 after therapy in both the subcutaneous and renal capsule models, an increase on day 7 and a decrease after first week showing response to the therapy through the second week. The total flux increased on day 4 in the second cohort of mice that received 37 MBq (1 mCi) of [^{131}I]mIBG and then showed a decrease until the second week in the subcutaneous models. In the renal capsule models, however, the total flux increased on day 7 and then showed a decrease until the second week. Moreover, the xenograft cohorts that received higher dose of MIBG showed comparatively greater change in total flux, i.e, the 2 mCi cohort showed greater response to therapy as compared to the 1 mCi cohort. In the control groups of both the models, there was observable increase in the total flux after the first day of therapy.

Animal Imaging and Tumor Uptake

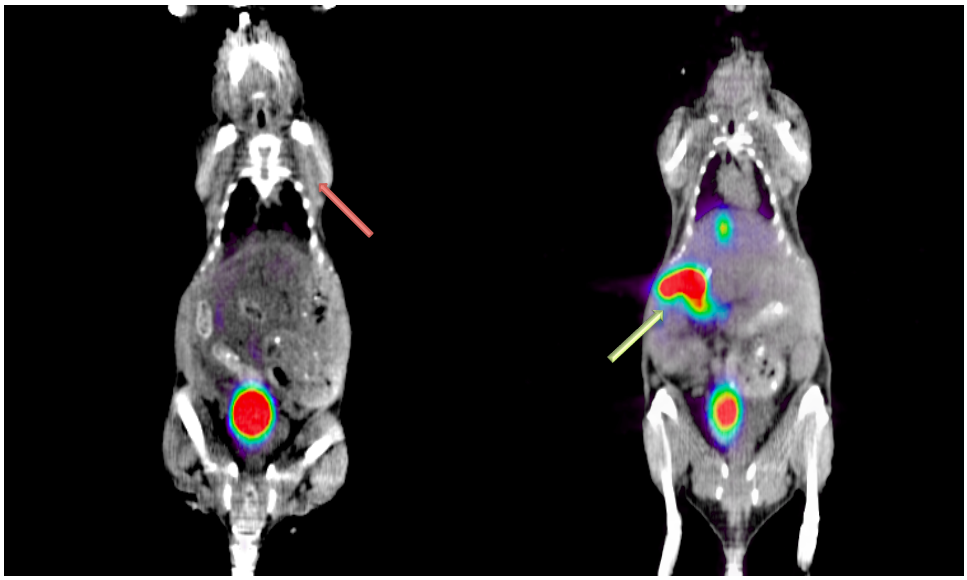

Figure 11: PET/CT images of subcutaneous model and renal capsule model (Red arrow indicates the location of the tumor in subcutaneous model (left) and Green arrow indicates the uptake in the abdominal organs surrounding the renal capsule (bottom) tumor)

There was no detectable [^{18}F]RP-109 uptake in subcutaneous xenografts of NB1691-luc-hNET cells and minimal uptake in the abdominal organs in the renal capsule xenografts of NB1691-luc-hNET cells (Figure 11). Tumor growth in the renal capsule xenografts was comparatively slower than with subcutaneous tumors, making simultaneous visualization of both large subcutaneous and large renal capsule tumors difficult. However, when large NB1691-hNET renal capsule tumors were established alone, clear uptake of [^{18}F]RP-109 was visualized in the abdominal organs. The Time Activity Curve (TAC) of both the models shows the distribution pattern (SUV) of [^{18}F]RP-109 in mice with time (Figure 12).

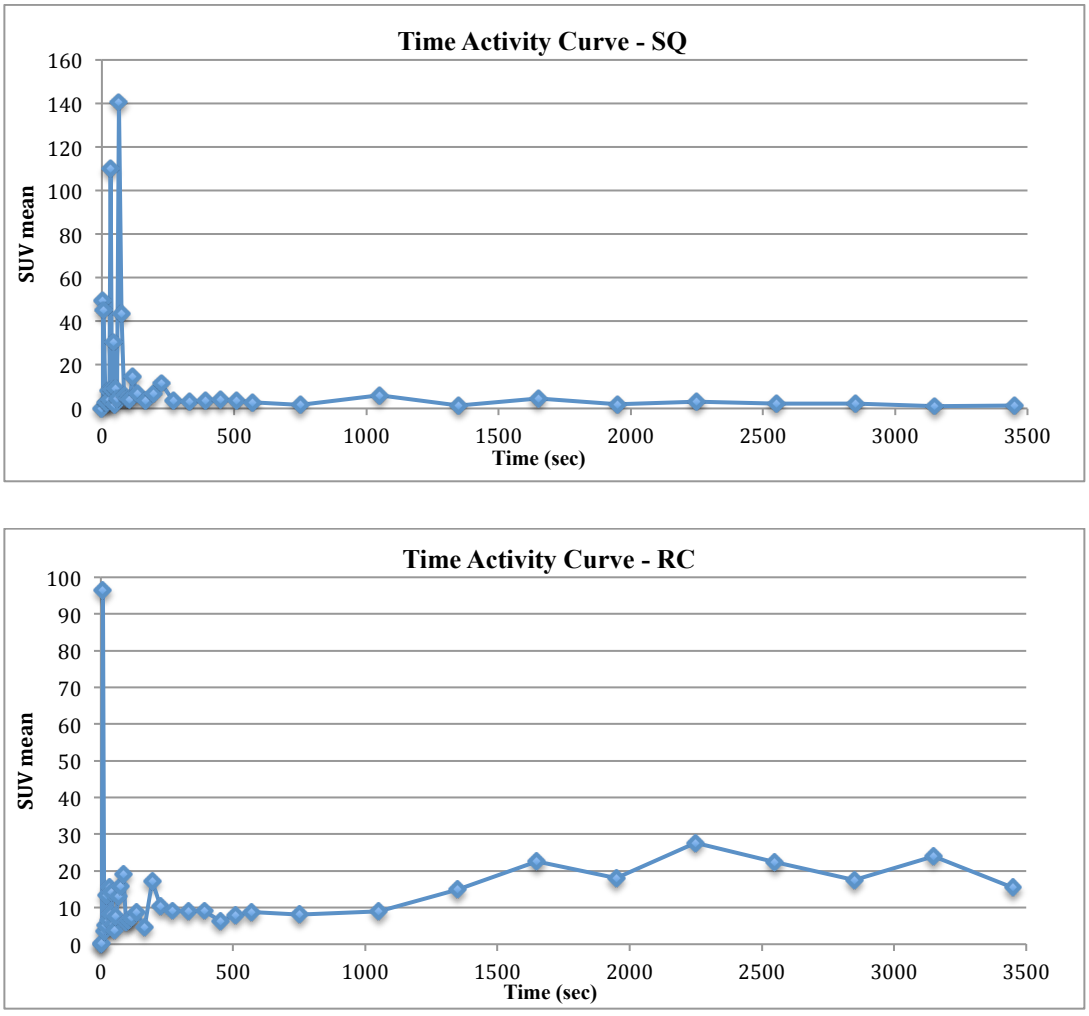

Figure 12: Time Activity Curve (TAC) of subcutaneous (top) and renal capsule (bottom) models

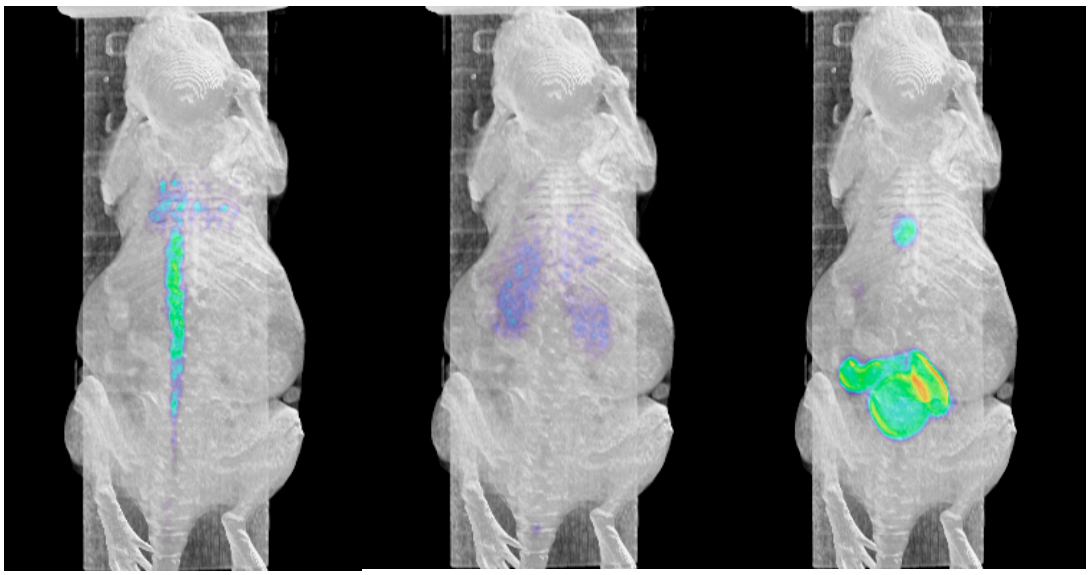

Figure 13: 3D rendered PET/CT images of subcutaneous model showing the uptake of the tracer at different time frames (2.5 sec, 135 sec, 3450 sec)

Statistical Analysis

Statistical analyses performed using Excel spreadsheets shows the data as average ± standard deviation (SD). The unpaired t-test shows statistical significance for the tumor volume change between the 2mCi and 1mCi cohorts with a P value of 0.002 and between the 2mCi and 0mCi cohorts with a P value of 0.004. Moreover, the total flux change for the subcutaneous model was statistically significant between the 2mCi and 1mCi cohorts with a P value of 0.0001; 2mCi and 0mCi cohorts with a P value of 0.010. For the renal capsule model, the total flux change was statistically significant with a P value of 0.0001 between 2mCi and 1mCi cohorts as well as between 2mCi and 0mCi cohorts.

Discussion

We have shown in this study that the novel probe, [^{18}F]RP-109, has been successfully synthesized and evaluated in neuroblastoma. The preliminary results shows that there was no quantifiable uptake of this novel probe in the subcutaneous

models but there was a slight uptake in the abdominal organs in the renal capsule models, indicating no correlation of [^{18}F]RP-109 with the neuroblastoma tumor cell NET expression.

We have demonstrated that the human neuroblastoma cell line transduced with hNET to overexpress the norepinephrine transporter is a reliable predictor of mIBG therapy. The data from this study shows similarity with the data from the previous study [5]. The treatment of neuroblastoma in murine xenograft model with [^{131}I]mIBG therapy showed a better response with bigger size tumors (>200 mm^3) and also with higher dose of [^{131}I]mIBG. The data from 1 mCi cohort and the data from 0 mCi cohort are indistinguishable, suggesting that 1 mCi dose has no therapeutic effect, whereas the data from 2 mCi cohort shows a response to therapy, indicating that it is a therapeutic dose for administration into the neuroblastoma. The data shows the effect of the therapy for a period of two weeks and there is relapse after two weeks.

We have demonstrated that the therapeutic data obtained from the bioluminescence imaging helps to assess the effectiveness of [^{131}I]mIBG treatment of neuroblastoma model and evaluate the functional status of tumors. The total flux obtained from the bioluminescence images shows that the viability of the neuroblastoma cells decreases after therapy and then there is unpredictable relapse. The data obtained from the caliper measurements also show the same trend, indicating the response to mIBG therapy. Moreover, all the statistical data shows P value less than 0.05 when comparing the tumor volumes and the total flux change, indicating statistical significance.

The human neuroblastoma cell line transduced with hNET to overexpress the norepinephrine transporter is a reliable *in vivo* model for mIBG therapy in both the subcutaneous and renal capsule model. These two xenograft models confirm the importance of hNET overexpression for strong *in vivo* mIBG uptake and, more importantly, allow the establishment of an *in vivo* model system with strong uptake necessary for radiation dosimetry and therapeutic preclinical trials [5]. The question that arises is that whether this experimental approach using [^{18}F]RP-109 in animal models of neuroblastoma will be useful in the clinical translation to improve mIBG therapy regimen.

We have noticed certain limitations of this study. We were unsure about the uptake of the novel probe in both the models. There is no conclusive reason for non-uptake in the tumor cells and it needs further investigation. A question that arises is if the hNET in neuroblastoma tumors is the same as the NET that has previously been evaluated in the brain of the monkey model. Since there is no evidence in the literature, which states that the hNET in neuroblastoma is different from the NET in the brain, so we could not speculate any reason for non-uptake.

Furthermore, in order to improve the efficacy of this targeted radionuclide therapy, investigators have tested increasing the dose by combining this therapy agent with standard cytotoxic agents. The remaining challenges will be to determine when to introduce them during therapy, whether in the neo-adjuvant setting, consolidation, or to treat minimal residual disease.

Conclusion

We have demonstrated that a novel probe has been successfully synthesized for evaluation in neuroblastoma. The preliminary results shows that there was no quantifiable uptake of [^{18}F]RP-109 in the xenograft models. There was no proper assessment of the tumors due to the failure of uptake, so the mIBG therapy was based on the tumor volume measurements using caliper. We have shown that the xenograft models of neuroblastoma responded only to the 2mCi dose of [^{131}I]mIBG therapy based on the data obtained from the bioluminescence imaging and caliper measurements. On the whole, we concluded that the therapeutic data is beneficial to assess the effect of mIBG therapy of neuroblastoma in the murine xenograft models overexpressing hNET. The development of the neuroblastoma xenograft models with in vivo uptake acts as a preclinical platform to evaluate mIBG treatment. The establishment of the animal model is a promising approach for evaluating radiation dosimetry and helps in the further exploration of therapy in combination with new drug candidates and radiosensitizers.

References:

1. Goodman M, Gurney J, Smith M, Olshan A, et al. Sympathetic Nervous System Tumors. In: Ries L, Smith M, Gurney J, et al., editors. Cancer Incidence and Survival among Children and Adolescents: United States SEER Program 1975–1995. Bethesda: National Institutes of Health: National Cancer Institute, SEER Program; 1999. pp. 65–72

2. Mathay, K. K., George, R. E., Yu, A. L. Promising therapeutic targets in neuroblastoma*. Clin. Cancer Res.* **18**, 2740- 2753 (2012)

3. Braden, M., Rider, K., Zheng, M. Q., Weinzimmer, D., Gerdes, J. From molecular to kinetic modeling: discovery and development of a novel class of Norepinephrine Transporter PET tracers. *J. Nucl. Med*. **52(S1),** 312(2011)

4. Zheng, M. Q., Gerdes, J. M., Weinzimmer, D., Ahmed, S., Braden, M et al. A new F-18 labeled PET tracer for the norepinephrine transporter. *J. Nucl. Med.* **53(S1),** 75 (2012)

5. Seo Y., Gustafson W.C., Dannoon S.F., Nekritz E.A., Lee C.L., Murphy S.T., VanBrocklin H.F., Hernandez- Pampaloni M., Haas-Kogan D.A., Weiss W.A., Matthay K.K. Tumor dosimetry using [124I]m-iodobenzylguanidine microPET/CT for [131I]m-iodobenzylguanidine treatment of neuroblastoma in a murine xenograft model *Mol Imaging Biol.* 2012 Dec;14(6):735-42. doi: 10.1007/s11307-012-0552-4

6. Voss, s. D., Smith, S. V., DiBartolo, N., Mcintosh, L., Cyr, E. M. et al. Positron emission tomography(PET) imaging of neuroblastoma and melanoma with ^{64}Cu-sarAr immunoconjugates *Proc. Natl. Acad. USA* **104**, 17489-17493 (2007)

7. Zhang H., Huang R., Lewis J., Blasberg R., Imaging human norepinephrine transporter (hNET) expressing reporter cells and tumors with 4-^{18}F-Fluorobenzylguanidine *J Nucl Med.* 2012; 53 (Supplement 1):1584

8. Yang, R.K, Sondel, P.M. Anti-GD2 Strategy in the Treatment of Neuroblastoma *Drugs Future.* 2010;35(8):665

9. DuBois SG, Matthay KK (2008) Radiolabeled metaiodobenzylguanidine for the treatment of neuroblastoma. Nucl Med Biol 35(Suppl 1): S35–S48

10. Smith, G. E., Sladen, H.L., Biagini, S. C. G., Blower, P. J. Inorganic approaches for labeling biomolecules with fluorine-18 for imaging with Positron Emission Tomography. *Dalton T.***40**, 6196-6205(2011)

Publishing Agreement

It is the policy of the University to encourage the distribution of all theses, dissertations, and manuscripts copies of all UCSF theses, dissertations, and manuscripts will be routed to the library via the Graduate Division. The library will make all theses, dissertations, and manuscripts accessible to the public and will preserve these to the best of their ability, in perpetuity.

Please sign the following statement:

I hereby grant permission to the Graduate Division of the University of California, San Francisco to release copies of my thesis, dissertation, or manuscript to the Campus Library to provide access and preservation, in whole or in part, in perpetuity.

Rupinder Kaur — 09-10-2013

Author Signature — Date